Polarity mediates asymmetric trafficking of the Gβ heterotrimeric G-protein subunit GPB-1 in *C. elegans* embryos

Kalyani Thyagarajan, Katayoun Afshar and Pierre Gönczy*

SUMMARY

Asymmetric cell division is an evolutionarily conserved process that gives rise to daughter cells with different fates. In one-cell stage *C. elegans* embryos, this process is accompanied by asymmetric spindle positioning, which is regulated by anterior-posterior (A-P) polarity cues and driven by force generators located at the cell membrane. These force generators comprise two Gα proteins, the coiled-coil protein LIN-5 and the GoLoco protein GPR-1/2. The distribution of GPR-1/2 at the cell membrane is asymmetric during mitosis, with more protein present on the posterior side, an asymmetry that is thought to be crucial for asymmetric spindle positioning. The mechanisms by which the distribution of components such as GPR-1/2 is regulated in time and space are incompletely understood. Here, we report that the distribution of the Gβ subunit GPB-1, a negative regulator of force generators, varies across the cell cycle, with levels at the cell membrane being lowest during mitosis. Furthermore, we uncover that GPB-1 traffics through the endosomal network in a dynamin- and RAB-5-dependent manner, which is most apparent during mitosis. We find that GPB-1 trafficking is more pronounced on the anterior side and that this asymmetry is regulated by A-P polarity cues. In addition, we demonstrate that GPB-1 depletion results in the loss of GPR-1/2 asymmetry during mitosis. Overall, our results lead us to propose that modulation of Gβ trafficking plays a crucial role during the asymmetric division of one-cell stage *C. elegans* embryos.

KEY WORDS: *C. elegans*, Asymmetric spindle positioning, Heterotrimeric G proteins, Intracellular trafficking, Endosomes

INTRODUCTION

Asymmetric cell divisions allow daughter cells to adopt their proper fate during development and in stem cell lineages. Asymmetric divisions require the localization of fate determinants along a polarity axis and the subsequent correct placement of the cleavage furrow to accurately segregate these determinants to daughter cells (reviewed by Gönczy, 2008; Knoblich, 2008). In animal cells, spindle positioning directs the placement of the cleavage furrow, which is specified so as to bisect the mitotic spindle. Therefore, deciphering the mechanisms that govern spindle positioning is crucial to achieve a thorough understanding of asymmetric cell division.

The one-cell stage *C. elegans* embryo is well suited for investigating spindle positioning during asymmetric cell division (reviewed by Gönczy, 2008). Here, asymmetric spindle positioning results from unequal net pulling forces acting on the two spindle poles during mitosis, with more force pulling on the posterior side (Grill et al., 2001). These pulling forces reflect the action of evolutionarily conserved force generators located at the cell membrane, which anchor dynein and act on the plus end of astral microtubules (Couwenbergs et al., 2007; Grill et al., 2003). In *C. elegans*, these force generators comprise the partially redundant heterotrimeric Gα proteins GOA-1 and GPA-16, the essentially identical GoLoco proteins GPR-1 and GPR-2 (hereafter referred to as GPR-1/2), and the coiled-coil domain protein LIN-5 (Colombo

et al., 2003; Couwenbergs et al., 2007; Gönczy et al., 2000; Gotta and Ahringer, 2001; Gotta et al., 2003; Nguyen-Ngoc et al., 2007; Park and Rose, 2008; Srinivasan et al., 2003; Tsou et al., 2003). Available evidence suggests that the posterior enrichment of GPR-1/2 and perhaps LIN-5 is responsible for generating the larger net pulling force on the posterior spindle pole during mitosis (Colombo et al., 2003; Gotta et al., 2003; Park and Rose, 2008; Tsou et al., 2003).

The mechanisms by which force generators are modulated in time and space in one-cell stage *C. elegans* embryos are incompletely understood. Although it is clear that anterior-posterior (A-P) polarity cues established by the PAR proteins act as upstream regulators of GPR-1/2 asymmetric enrichment (Colombo et al., 2003; Gotta et al., 2003; Park and Rose, 2008; Tsou et al., 2003), the means by which this regulation is achieved is not entirely clear. This is despite the knowledge of some components that regulate the presence of GPR-1/2 at the cell membrane. Thus, the two Gα subunits together are crucial for the recruitment of GPR-1/2 to the cell membrane (Colombo et al., 2003), and the PP6 phosphatase PPH-6 as well as its partner SAPS-1 also contribute to this recruitment (Afshar et al., 2010). Moreover, the casein kinase CSNK-1 is a negative regulator of overall GPR-1/2 levels at the cell membrane (Panbianco et al., 2008), whereas the DEP domain protein LET-99 is important for restricting the domain on the cell membrane to which GPR-1/2 is enriched (Panbianco et al., 2008; Tsou et al., 2003).

Another important modulator of force generators is the Gβγ complex of heterotrimeric G proteins, which consists of the Gβ protein GPB-1 and the Gγ protein GPC-2 (Afshar et al., 2005; Gotta and Ahringer, 2001; Tsou et al., 2003). Depletion of GPB-1 by RNAi results in higher net pulling forces on the anterior spindle pole, indicating that Gβ is a negative regulator of force generators

Swiss Institute for Experimental Cancer Research (ISREC), School of Life Sciences, Swiss Federal Institute of Technology (EPFL), Lausanne CH-1015, Switzerland.

*Author for correspondence (pierre.gonczy@epfl.ch)

on the anterior side during mitosis (Afshar et al., 2004). Moreover, embryos depleted of GPB-1 or GPC-2 exhibit exaggerated movements of centrosomes and associated pronuclei prior to mitosis and consequently have defects in pronuclear centration (Afshar et al., 2004; Tsou et al., 2003). Overall levels of GPR-1/2 at the cell membrane are higher than is normal at that stage in such embryos (Afshar et al., 2004; Tsou et al., 2003), indicating that Gβ acts as a negative regulator of GPR-1/2 cell membrane accumulation. Although GPB-1 is enriched at the cell membrane of two- and four-cell stage embryos (Gotta and Ahringer, 2001; Zwaal et al., 1996), its distribution across the first cell cycle has not been investigated previously. As a result, it is not known to what extent the modulation of Gβγ distribution may be harnessed to regulate force generators in one-cell stage embryos.

Heterotrimeric G protein assembly and delivery to the cell membrane have been extensively studied in mammalian cells (reviewed by Marrari et al., 2007). G protein subunits are synthesized on free ribosomes in the cytoplasm, after which the Gα and Gγ subunits are modified by the addition of a lipid tail to each, allowing their association with intracellular membranes. The Gβ subunit forms a tight complex with the Gγ subunit, and the Gβγ complex then associates with Gα subunits to form the heterotrimer. Classically, heterotrimeric G proteins function downstream of G protein-coupled receptors that span the cell membrane. Whereas it was initially believed that the heterotrimeric complex always remains associated with the cell membrane, it has been suggested that, in mammalian cells, the subunits can translocate from the cell membrane to the cytosol and thereafter associate with intracellular compartments (Allen et al., 2005; Chisari et al., 2007; Garcia-Regalado et al., 2008; Hynes et al., 2004; Saini et al., 2007). Whether a similar process occurs in early *C. elegans* embryos and whether its regulation might have a role in modulating asymmetric spindle positioning forces have not previously been addressed.

In this study we investigated the possibility that the temporal and spatial regulation of Gβγ plays a role in asymmetric spindle positioning. Our work reveals that endosomal trafficking regulates GPB-1 distribution in one-cell stage *C. elegans* embryos both in time and space and is crucial for ensuring the asymmetric distribution of GPR-1/2 during mitosis.

MATERIALS AND METHODS
Nematode strains and RNAi
Transgenic worms expressing GFP-RAB-5 (Sato et al., 2008), GFP-RME-1 (Balklava et al., 2007) as well as GFP-GPB-1 and GFP-GPC-2 (this study) were maintained at 24°C. mCherry-RAB-5Q78L transgenic animals (Audhya et al., 2007) were maintained at 15°C, as were *dyn-1(ky51)* animals (Clark et al., 1997) obtained from the *Caenorhabditis* Genetics Center. For *par-3(it71)* (Cheng et al., 1995), worms were shifted to 25°C for 20-25 hours prior to analysis. For acute dynamin inactivation, *dyn-1(ky51)* or wild-type control animals were transferred to 10 µl water in a PCR tube and kept for 3 minutes at ~26.5°C in a water bath, before being dissected and processed for immunofluorescence. *dyn-1(ky51)* animals exhibited the reported paralysis phenotype (Clark et al., 1997) after this 3-minute shift. However, we did not observe the late cytokinesis phenotype reported by Thompson and colleagues, even after 40 hours at 25°C (Thompson et al., 2002). Identical results were obtained with a separate isolate of *dyn-1(ky51)* obtained from Cori Bargmann (Clark et al., 1997).

Transgenic lines expressing GFP-GPB-1 and GFP-GPC-2 were generated by cloning full-length cDNAs obtained by RT-PCR into the germline expression vector pSU25 (Bellanger and Gönczy, 2003). The plasmids were verified by sequencing and bombarded (Praitis et al., 2001). For GFP-GPB-1, we obtained two integrated lines (GZ789 and GZ790) with similar expression levels, and GZ789 was used for this study. For

GFP-GPC-2, we obtained one integrated line (GZ963) and one non-integrated line (GZ967). Although the non-integrated line showed brighter GFP expression, we used the integrated line to avoid variation in expression levels between embryos. For monitoring the association of GPB-1 with early endosomes, GFP-GPB-1 males were crossed with mCherry-RAB-5Q78L hermaphrodites, and embryos from the F1 generation were analyzed.

The *gpc-2(RNAi)*, *dyn-1(RNAi)* and *rab-5(RNAi)* feeding strains were obtained from the ORFeome RNAi library (gift from Jean-François Rual and Marc Vidal, Harvard Medical School, Boston, MA, USA). To obtain the feeding strain for *gpb-1(RNAi)*, a genomic region encompassing exons 6 and 7 of *gpb-1* was amplified and subcloned into L4440 (Timmons and Fire, 1998) and subsequently transformed into HT115 bacteria. RNAi was performed by feeding L3-L4 animals at 25°C for 25 hours for *gpb-1(RNAi)* and *gpc-2(RNAi)*, at 20°C for 22-24 hours for *dyn-1(RNAi)*, and at 24°C for 20-24 hours for *rab-5(RNAi)*.

Antibody production and indirect immunofluorescence
GPB-1 antibodies were produced by cloning full-length *gpb-1* cDNA into pGEX-6P2 (Promega), expressing GST-GPB-1 and purifying it from inclusion bodies. The protein was gel purified and injected into a rabbit (Eurogentec). The resulting antibodies were strip-purified against GST-GPB-1, using 0.1 M glycine pH 2.5 as an elution buffer. Affinity-purified antibodies were then dialyzed against PBS and kept at –20°C in 50% glycerol at 0.2 mg/ml. By western blot, these antibodies detect essentially a single band at the expected size, which is significantly diminished upon *gpb-1(RNAi)* (see Fig. S1 in the supplementary material), and by immunofluorescence exhibit a distribution analogous to that of previously reported GPB-1 antibodies (Zwaal et al., 1996).

For immunostaining, embryos were fixed in methanol at –20°C for 1 hour (GPB-1 staining) or 15 minutes (GPR-1/2 staining) followed by overnight incubation with primary antibodies at 4°C. Primary mouse antibodies against α-tubulin (1/300; DM1A, Sigma) and GFP (1/50; MAB3580, Millipore) were used together with rabbit antibodies against GPB-1 (1/200; this study) or GPR-1/2 [1/100 (Afshar et al., 2010)]. Secondary antibodies were Alexa 488-conjugated goat anti-mouse (1/500; Molecular Probes) and Cy3-conjugated goat anti-rabbit (1/1000; Dianova). Slides were counterstained with 1 mg/ml Hoechst 33258 (Sigma) to visualize DNA. Images were acquired on an LSM700 confocal microscope (Zeiss) and processed in ImageJ and Adobe Photoshop, maintaining relative image intensities.

Microscopy and image analysis
For quantification of embryos immunostained with GPB-1 and GPR-1/2 antibodies, images were acquired on the LSM700 using a 63× objective, zoom 2, average 4 and unidirectional scanning of 1024×1024 pixels at 2% laser power and a pinhole of 1 airy unit to give an image thickness of 0.7 µm. For quantification of cortical to cytoplasmic ratio, the total fluorescence intensity was measured using ImageJ in an area with an average width of ~1 µm drawn around the anterior or posterior cortex. The same area was used to measure fluorescence intensity in the cytoplasm, and the ratio of cortical to cytoplasmic intensities was computed. For cortical to cytoplasm ratio measurements of GFP-GPB-1 in live embryos (see Movie 1 in the supplementary material), images were captured on the LSM700 every 20 seconds using a 40× objective, zoom 2, average 8, and unidirectional scanning of 512×512 pixels at 2% laser power with a fully open pinhole to give an image thickness of 12.5 µm. Movies were processed using a custom-designed MetaMorph journal to calculate the average fluorescence intensity of the entire cell cortex and of a similar region in the cytoplasm for every frame.

For the FM 4-64 (SynaptoRed C2, Biotium) experiments (see Movie 2 in the supplementary material), a laser microdissection microscope (LMD, Leica) was used to pierce a hole in the eggshell of GFP-GPB-1 embryos (Nguyen-Ngoc et al., 2007) bathed in a 32 µM solution of FM 4-64 dye. Embryos were then imaged at the LSM 700 every 10 seconds using a 63× objective, zoom 1.5, average 4, and unidirectional scanning of 512×512 pixels at 2% laser power with a pinhole of 1 airy unit to give an image thickness of 0.7 µm. Identical conditions were used to image embryos
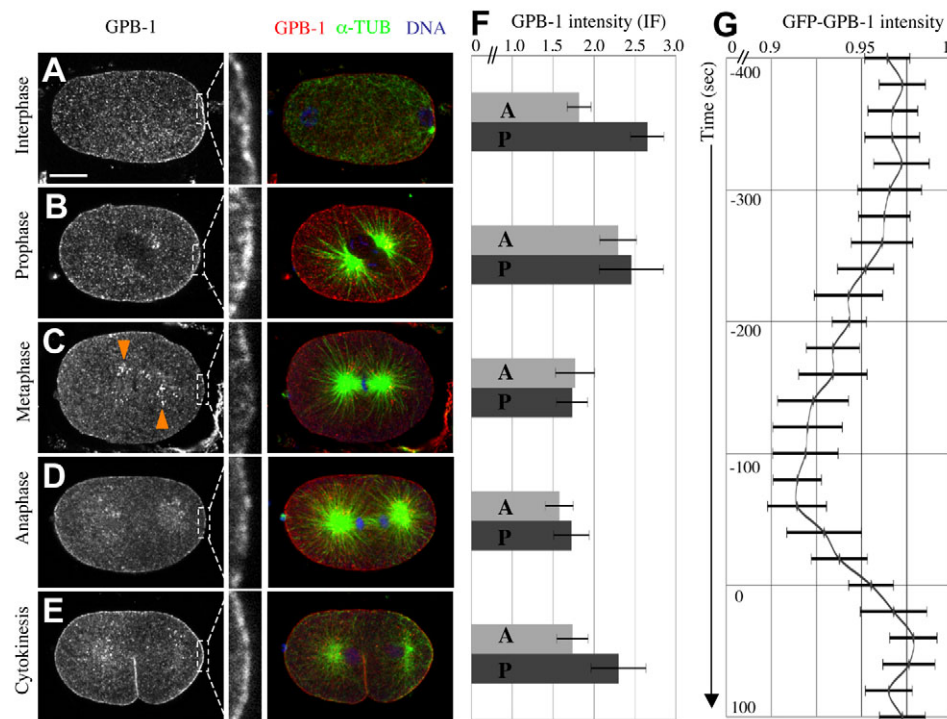
Fig. 1. GPB-1 cell membrane distribution fluctuates during the cell cycle. (**A-E**) Wild-type *C. elegans* embryos stained for GPB-1 (shown alone in left panels and in red in merges) and α-tubulin (green); DNA is stained with DAPI (blue) in this and other figures. Boxed regions are magnified to display GPB-1 at the cell membrane. Arrowheads indicate accumulation of GPB-1 around the asters. Note that for simplicity, prometaphase and metaphase embryos are designated collectively as metaphase embryos. Scale bar: 10 µm. (**F**) Ratio of cortical to cytoplasmic GPB-1 at the anterior (A) and posterior (P) cell membrane in fixed embryos. Error bars represent s.e.m. For actual values and statistical analysis, see Table S1 in the supplementary material. (**G**) GFP-GPB-1 cortical to cytoplasmic ratio from confocal recordings of live embryos ($n=9$). $t=0$ corresponds to the onset of cleavage furrow formation; metaphase is approximately at $t=-140$ seconds. See Movie 1 in the supplementary material.

expressing GFP-GPB-1 and mCherry-RAB-5Q78L (see Movie 5 in the supplementary material). For Movie 3 in the supplementary material, images were acquired every 2 seconds with 300 msecond exposure using a 63× objective at the spinning disc confocal microscope, essentially as described (Bellanger and Gönczy, 2003).

Fluorescence recovery after photobleaching (FRAP) was performed on the LSM700. For FRAP of the membrane and astral pool at the four cell stage (see Movie 4 in the supplementary material), a region covering the entire cortex of one of the four cells, together with a circular region covering the entire astral pool, was bleached with two iterations at 100% laser power and images acquired every 500 mseconds using a 40× objective, zoom 2.2, average 8 and bidirectional scanning of 512×512 pixels with a pinhole opened to acquire a section 2 µm thick. For cortical FRAP at the one cell stage (see Movie 6 in the supplementary material), a square at the anterior or posterior cortex was bleached with ten iterations at 100% laser power and images acquired every second using a 40× objective, zoom 2, average 1 and bidirectional scanning at 256×256 pixels, with the pinhole opened to acquire a section 4 µm thick. For FRAP at the cell-cell boundary at the two cell stage (see Movie 7 in the supplementary material), a region covering the entire cell-cell boundary was bleached with 15 iterations at 100% laser power and images acquired every second using a 63× objective, zoom 2, average 2 and bidirectional scanning of 512×512 pixels, with a fully open pinhole resulting in an optical section of 7.4 µm thickness. The maximum intensity observed in the frames before photobleaching was assigned a value of 1, and that in the bleached area just after photobleaching a value of 0. Other intensities were normalized with respect to these values.

RESULTS

GPB-1 distribution varies across the cell cycle in one-cell stage embryos

We set out to investigate in detail the distribution of GPB-1 in one-cell stage embryos to better understand how Gβγ might regulate GPR-1/2 localization during asymmetric cell division. As shown in Fig. 1A-F and Table S1 in the supplementary material, immunofluorescence analysis revealed that GPB-1 distribution varies across the cell cycle. During interphase, GPB-1 is more enriched at the cell membrane on the posterior than on the anterior

side (Fig. 1A,F). Thereafter, GPB-1 levels at the cell membrane are uniform during prophase (Fig. 1B,F). Interestingly, during metaphase and anaphase (hereafter referred to collectively as mitosis, for simplicity), levels of cell membrane GPB-1 are lower than at preceding stages of the cell cycle (Fig. 1C,D,F). During cytokinesis, GPB-1 cell membrane levels are higher again, especially on the posterior side of the embryo (Fig. 1E,F).

Gβ subunits lack membrane targeting signals but are known in other systems to associate with Gγ subunits that have a lipid tail, which serves to insert the Gβγ complex into membranes (Marrari et al., 2007). Accordingly, we found that GPB-1 requires the Gγ subunit GPC-2 to reach the cell membrane in *C. elegans* embryos (see Fig. S2A,B in the supplementary material). Moreover, we generated transgenic lines expressing GFP-GPC-2, which was also enriched at the cell membrane in early embryos (data not shown). These results indicate that GPB-1 can be used as a marker for the distribution of the Gβγ complex as a whole.

We addressed whether the reduction in GPB-1 at the cell membrane during mitosis observed in fixed specimens could be recapitulated in live embryos. We generated transgenic lines expressing GFP-GPB-1, which was distributed in a manner essentially indistinguishable from endogenous GPB-1 (see Fig. S2C in the supplementary material). Quantification of time-lapse recordings of one-cell stage embryos revealed that levels of cell membrane GFP-GPB-1 are lower during mitosis (Fig. 1G; see Movie 1 in the supplementary material). Together, these observations uncover a hitherto unknown temporal regulation of GPB-1 in one-cell stage *C. elegans* embryos in which levels at the cell membrane are lower during mitosis than at other stages of the cell cycle.

GPB-1 traverses the endosomal system

Our analysis of fixed specimens also revealed an enrichment of discrete GPB-1 punctae around the microtubule asters, especially during mitosis (Fig. 1C, arrowheads). Accumulation in the vicinity of asters has been reported previously in later stage embryos

(Zwaal et al., 1996), but not investigated further. We set out to determine the nature of the intracellular compartment in which GPB-1 localizes during mitosis.

We found that intracellular GFP-GPB-1 colocalizes with structures marked by the lipophilic dye FM 4-64, which labels the plasma membrane and endosomes (Vida and Emr, 1995), indicating that intracellular GPB-1 is associated with endosomal compartments (Fig. 2A and see Movie 2 in the supplementary material). We reasoned that if GPB-1 indeed traverses the endosomal network, then GFP-GPB-1 should be observed on mobile intracellular vesicles. Accordingly, in addition to the signal at the plasma membrane (Fig. 2B, left panel, arrowhead), live imaging of the midplane of the embryo revealed GFP-GPB-1-positive intracellular vesicle-like structures (Fig. 2B, right panel, arrowheads; see Movie 3 in the supplementary material). These structures were often mobile and moved in a straight path towards the asters (Fig. 2C; see Movie 3 in the supplementary material). Additionally, if intracellular GPB-1 is associated with the endosomal network, another prediction is that this protein pool should not exchange readily with that in the cytoplasm. To test this prediction, we conducted fluorescence recovery after photobleaching (FRAP) experiments with embryos expressing GFP-GPB-1. As shown in Fig. 3A and Movie 4 in the supplementary material, we found that the intracellular signal indeed does not recover readily after photobleaching, in contrast to the signal at the plasma membrane (see also below).

To uncover the nature of the endosomal compartments in which GPB-1 resides during mitosis, we addressed whether GPB-1 colocalizes with the early endosomal marker RAB-5, given that early endosomes accumulate around the asters during this stage of the cell cycle (Andrews and Ahringer, 2007). We found that many of the GPB-1 punctae indeed colocalize with GFP-RAB-5 (Fig. 2D). Accordingly, live imaging revealed a close association between GFP-GPB-1 and early endosomal vesicles marked by mCherry-RAB-5Q78L (Fig. 2E, arrowheads; see Movie 5 in the supplementary material). Interestingly, in addition, we found significant colocalization in fixed specimens between GPB-1 and GFP-RME-1, a marker of recycling endosomes (Fig. 2F).

Overall, these experiments establish that GPB-1 is present in early and recycling endosomes during mitosis in one-cell stage *C. elegans* embryos. Hereafter, we refer to this pool of GPB-1 as the endosomal pool and movement within this pool as GPB-1 trafficking.

GPB-1 at the cell membrane is dynamic

The transient reduction in GPB-1 at the cell membrane and concomitant accumulation in endosomes during mitosis suggests that a fraction of the plasma membrane pool is mobile, so as to be able to enter the endosomal network. We conducted FRAP experiments to address this prediction, photobleaching GFP-GPB-1 at the cell membrane in one-cell and two-cell stage embryos. We found that the cell membrane signal recovers rapidly, with a $t_{1/2}$ of ~5 seconds (Fig. 3B-D; see Movies 6 and 7 in the supplementary material). This recovery appeared to be from the intracellular milieu and not from lateral diffusion within the cell membrane, as recovery was uniform throughout the bleached region of the plasma membrane (Fig. 3C; see Movie 6 in the supplementary material). Only ~60% of the initial signal recovered within the time span of the experiment (Fig. 3D), indicating that ~40% of plasma membrane GFP-GPB-1 is significantly less mobile. Furthermore, the kinetics of rapid GFP-GPB-1 recovery was similar at different stages of the cell cycle (see legend to Fig. 3). This indicates that the decrease in the cell membrane levels of GPB-1 during mitosis is not due to a difference
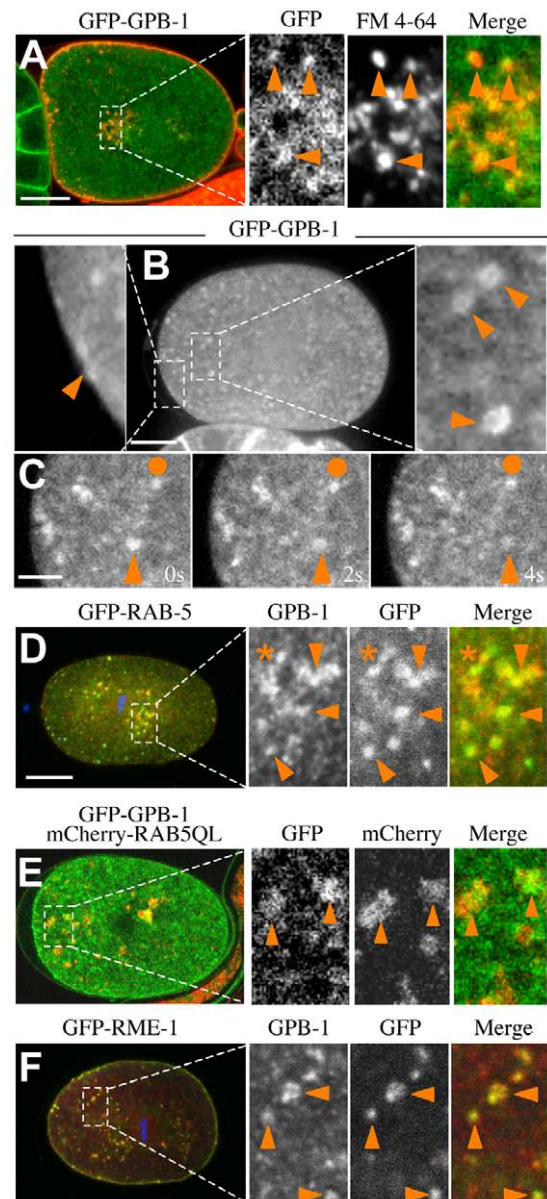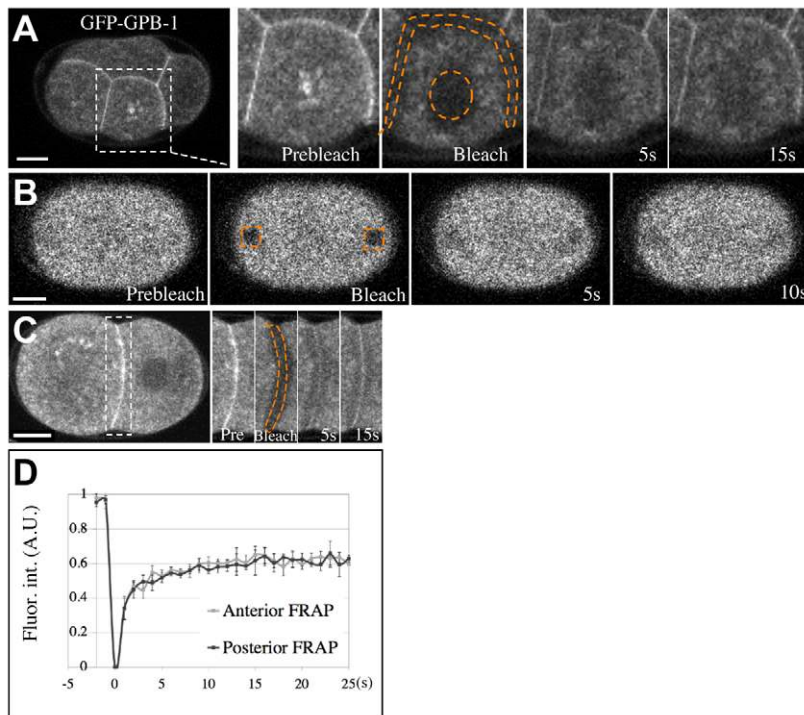

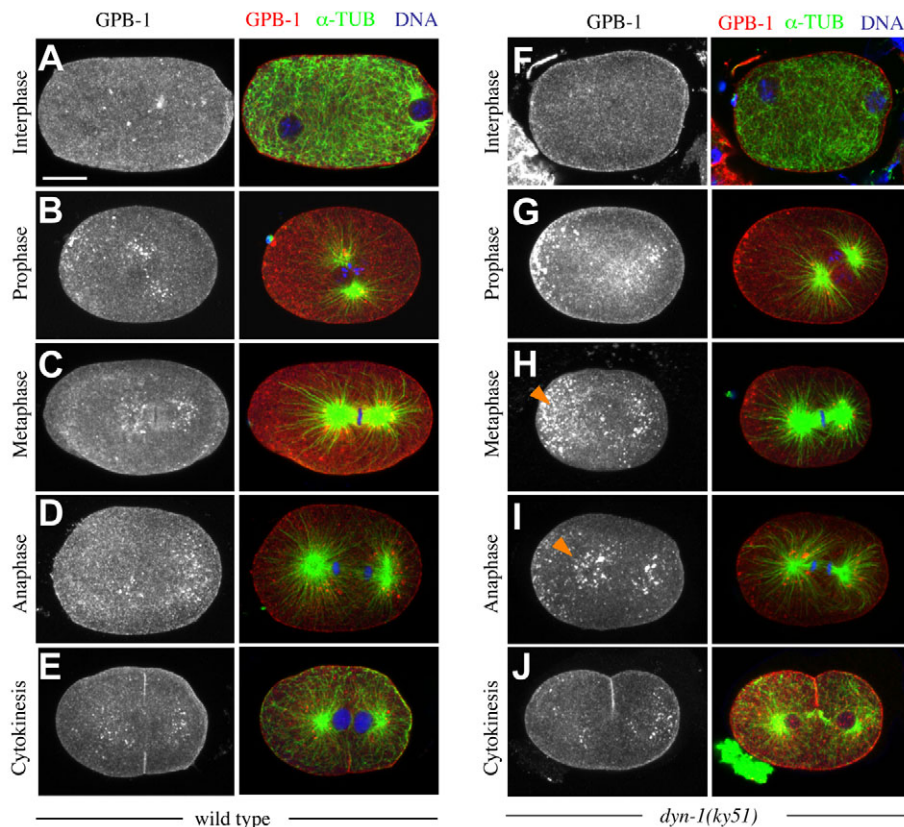**Fig. 2. GPB-1 associates with early and recycling endosomes.** (**A**) GFP-GPB-1 (green in merge) *C. elegans* embryo infused with FM 4-64 lipophilic dye (red in merge), showing colocalization, especially around the asters. The boxed region is magnified on the right and arrowheads point to colocalizing structures. See Movie 2 in the supplementary material. (**B**) GFP-GPB-1 is present on the cell membrane (magnified on the left, arrowhead) and in intracellular vesicles (magnified on the right, arrowheads) in live one-cell stage embryos (an embryo in mitosis is shown here). See Movie 3 in the supplementary material. (**C**) GFP-GPB-1 vesicle (arrowhead) moving towards the aster. The disc denotes a vesicle that is stationary within this sequence. Cell membrane is towards the left of each panel. (**D**) GFP-RAB-5 embryos stained for GPB-1 and GFP (red and green in merge, respectively). Arrowheads point to colocalizing structures. Note that colocalization is observed in the vicinity of the centrosomes (asterisk), as well as further away. (**E**) Embryos expressing GFP-GPB-1 and mCherry-RAB-5QL (green and red in merge, respectively). Arrowheads point to GFP-GPB-1- and mCherry-RAB-5QL-positive endosomes. See Movie 5 in the supplementary material. (**F**) GFP-RME-1 embryos stained for GPB-1 and GFP (red and green in merge, respectively). Arrowheads point to colocalizing structures. Scale bars: 10 μm in A,B,D; 5 μm in C.

Fig. 3. GFP-GPB-1 dynamics at the cell membrane. (**A**) Fluorescence recovery after photobleaching (FRAP) of endosomal and cell membrane pools of GFP-GPB-1 in a four-cell stage *C. elegans* embryo. Orange dashed lines indicate photobleached areas. Note the lack of signal recovery at the endosomal pool, in contrast to rapid recovery at the cell membrane. See Movie 4 in the supplementary material. (**B**,**C**) Photobleaching and recovery of the cell membrane pool of GFP-GPB-1 at the anterior and posterior cortex of a one-cell stage embryo during mitosis (the cortical plane of a metaphase embryo is shown here) (B), as well as at the cell-cell boundary of a two-cell stage embryo (C). *t*=0 corresponds to the end of the bleaching period. The boxed region in C is shown on the right. See Movies 6 and 7 in the supplementary material. (**D**) FRAP of GFP-GPB-1 at the cell membrane in one-cell stage embryos. The recovery curve represents the average of embryos photobleached at interphase (*n*=4), prophase (*n*=4) and metaphase (*n*=5). Note that the rapid recovery of signal is independent of the cell cycle stage and is equal at the anterior and posterior of the embryo. Fluorescence intensity is given in arbitrary units (A.U.). Error bars indicate s.d. Scale bars: 10 μm.

in internalization from the plasma membrane. Instead, this could occur at the level of association with the endosomal compartment or be due to alteration of the transit rates within the compartment. Overall, these findings indicate that a substantial fraction of GPB-1 at the cell membrane can be rapidly mobilized and could thus potentially enter the endosomal compartment.

GPB-1 endosomal association is maximal during mitosis

Conceivably, entry into the endosomal network could occur by endocytosis of cell membrane GPB-1 or instead by translocation from the cell membrane to the cytoplasm followed by intracellular attachment to endosomes. As shown in Fig. 4 and Fig. S3 in the

Fig. 4. Temporal regulation of GPB-1 intracellular accumulation revealed upon acute dynamin inactivation. (**A-J**) Wild-type (A-E) and *dyn-1(ky51)* (F-J) *C. elegans* embryos shifted to the restrictive temperature for 3 minutes before fixation and staining for GPB-1 (shown alone on the left and in red in merge) and α-tubulin (green in merge). Panels showing GPB-1 alone (left) are maximum intensity projections of several confocal sections. Arrowheads (H,I) indicate GPB-1 accumulation in vesicle-like structures. Scale bar: 10 μm.

supplementary material, we found that GPB-1 does not accumulate on the plasma membrane above wild-type levels following inactivation of the GTPase dynamin, which is required for endocytosis (reviewed by Praefcke and McMahon, 2004). Although we cannot rule out that a small amount of dynamin is still present and sufficient to lead to GPB-1 endocytosis, this observation suggests that GPB-1 internalization is dynamin independent and the protein is either internalized in a dynamin-independent manner or more likely enters the endosomal pathway from the cytoplasm, as has been suggested for heterotrimeric G protein subunits in human cells (Hynes et al., 2004).

The transient presence of GPB-1 in early and recycling endosomes during mitosis suggests that GPB-1 endosomal association is modulated over time in one-cell stage embryos, being maximal during mitosis. We reasoned that if this were the case, then disrupting endosomal trafficking early in the cell cycle should have less of an impact on GPB-1 intracellular accumulation than disrupting it during mitosis. To test this prediction, we made use of a rapidly inactivating temperature-sensitive mutant allele of dynamin, *dyn-1(ky51)* (Clark et al., 1997), as dynamin is also required for fission and fusion events within the endosomal pathway (reviewed by Praefcke and McMahon, 2004). In mammalian cells, acute inactivation of dynamin function by overexpression of a temperature-sensitive mutant leads to defects in endocytosis in less than 5 minutes (Damke et al., 1995). Therefore, we reasoned that short exposures of *dyn-1(ky51)* embryos to the restrictive temperature followed by immunofluorescence analysis should provide a snapshot of the extent of GPB-1 trafficking at each stage of the cell cycle (see Materials and methods). In addition, we reasoned that such short-term inactivation of dynamin function should not alter A-P polarity, which is also dynamin dependent (Nakayama et al., 2009), thus simplifying the interpretation of these experiments. As shown in Fig. 4, we found that the impact of acute dynamin inactivation on GPB-1 distribution varies across the cell cycle, with GPB-1 distribution being most affected during mitosis. Together, these findings indicate that GPB-1 is present in the early and recycling endosomal compartments preferentially during mitosis.

GPB-1 trafficking is asymmetric during mitosis

In addition to the temporal regulation of GPB-1 trafficking revealed by the above experiments, we noted that the intracellular accumulation of GPB-1 upon acute inactivation of dynamin is asymmetric, with more accumulation at the anterior, especially during mitosis (Fig. 4H,I, arrowheads). We also found an asymmetric mislocalization of GPB-1 in *dyn-1(RNAi)* embryos, albeit at all stages of the cell cycle, as would be anticipated from chronic depletion of dynamin (see Fig. S3 in the supplementary material). These findings are suggestive of more GPB-1 trafficking taking place on the anterior than on the posterior side of the embryo.

As an alternative means of addressing this possibility, we depleted RAB-5, which is required for early endosome function and is also enriched on the anterior side during mitosis (Andrews and Ahringer, 2007). If GPB-1 trafficking is indeed more pronounced on the anterior side, then disruption of early endosome function would be expected to affect GPB-1 distribution more on that side. Accordingly, we found that GPB-1 accumulates in intracellular punctae primarily in the anterior of *rab-5(RNAi)* embryos (Fig. 5B; see Fig. S4B in the supplementary material). Moreover, GPB-1 was systematically absent from the cell membrane at the anterior, whereas it was still present to some
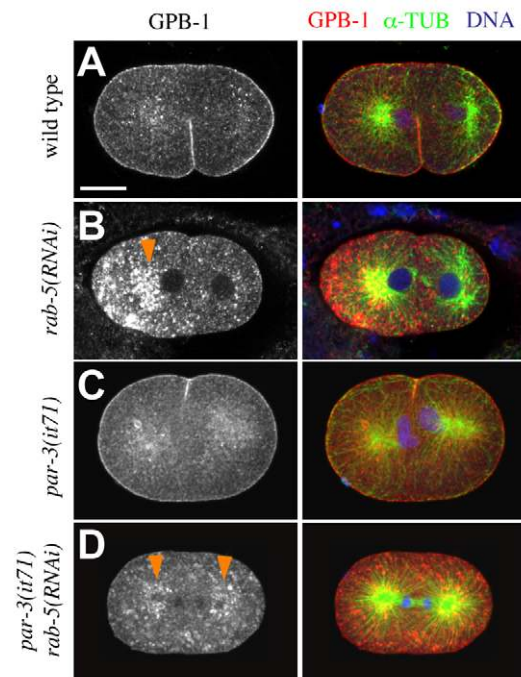

Fig. 5. Polarity cues regulate the asymmetry of GPB-1 trafficking. (**A-D**) GPB-1 localization in wild-type (A), *rab-5(RNAi)* (B), *par-3(it71)* (C) and *par-3(it71) rab-5(RNAi)* (D) one-cell stage *C. elegans* embryos during cytokinesis. Embryos are stained for GPB-1 (shown alone in left panels and in red in merges) and α-tubulin (green in merges). Arrowheads point to intracellular GPB-1 localization, which is anteriorly enriched in *rab-5(RNAi)* embryos and symmetrically distributed in *par-3(it71) rab-5(RNAi)* embryos. Scale bar: 10 µm.

extent at the posterior cell membrane (93% cytokinesis and two-cell stage embryos, *n*=73; Fig. 5B and see Fig. S4B in the supplementary material).

Together, these findings strongly support the view that GPB-1 trafficking in one-cell stage embryos is asymmetric during mitosis, being more pronounced on the anterior side. Compatible with this view, we found that wild-type embryos exhibit a posterior bias in the accumulation of intracellular GPB-1 punctae during mitosis (67% of embryos, with another 30% exhibiting uniform distribution; *n*=30). This suggests that GPB-1 trafficking is less effective on the posterior side in the wild type, thus resulting in more frequent accumulation in endosomal compartments.

Polarity regulates asymmetric GPB-1 trafficking

To address whether A-P polarity cues regulate such differential GPB-1 trafficking, we tested whether the asymmetric accumulation of GPB-1 observed in *rab-5(RNAi)* embryos is under the control of A-P polarity cues established by the PAR proteins. As shown in Fig. 5 and Fig. S4 in the supplementary material, the intracellular accumulation of GPB-1 was usually symmetric in *par-3(it71) rab-5(RNAi)*. We conclude that A-P polarity cues direct asymmetric GPB-1 trafficking and are thus important for the spatial regulation of GPB-1.

What could be the importance of the polarity-dependent regulation of GPB-1 trafficking? GPB-1 is a known negative regulator of GPR-1/2 levels at the cell membrane during prophase (Tsou et al., 2003) (see also Fig. 6B,G,K), as well as a negative regulator of pulling forces at the anterior during mitosis (Afshar et al., 2004). Therefore, the asymmetry in GPB-1 trafficking during

mitosis could be important for the asymmetric distribution of GPR-1/2 at the cell membrane. If this were the case, then GPR-1/2 asymmetry between the anterior and posterior sides should be lost upon GPB-1 depletion and lead to symmetric pulling forces. To address this possibility, we measured the ratio of GPR-1/2 cell membrane levels at the posterior versus the anterior, comparing wild-type with *gpb-1(RNAi)* and *gpb-1(RNAi) gpc-2(RNAi)* embryos [hereafter pooled and referred to collectively as *gpb-1(RNAi)* as there was no apparent difference between the two conditions]. Importantly, focusing on metaphase embryos, in which the asymmetry of GPR-1/2 is most apparent in the wild type (Fig. 6C,L), we found that GPR-1/2 distribution is symmetric in *gpb-1(RNAi)* embryos (Fig. 6H,L and see Table S2 in the supplementary material). Together, these findings lead us to propose that GPB-1 distribution plays a crucial role in imparting GPR-1/2 asymmetry during mitosis, thereby modulating asymmetric spindle positioning.

DISCUSSION

The accurate regulation of spindle positioning is crucial for proper asymmetric cell division, but how this is achieved remains poorly understood. In this study, we report that the Gβ protein GPB-1 is subject to temporal and spatial regulation in one-cell stage *C. elegans* embryos. Our findings lead us to propose that regulation of GPB-1 distribution by polarity-dependent asymmetric intracellular trafficking is crucial for proper GPR-1/2 distribution during mitosis and thus for spindle positioning during the asymmetric division of *C. elegans* embryos.

Gβ trafficking in early *C. elegans* embryos

Our work in *C. elegans* reveals that the pool of the Gβ subunit GPB-1 located at the cell membrane is mobile and also that GPB-1 associates with early and recycling endosomes. Association of heterotrimeric G protein components with endosomal compartments has been observed in mammalian cells in the context of their function in receptor-mediated signaling (Chisari et al., 2007; Garcia-Regalado et al., 2008; Hynes et al., 2004; Saini et al., 2007). Our work demonstrates that heterotrimeric G protein subunits are also very dynamic in the context of their role in asymmetric cell division, which is thought to be receptor independent (for reviews, see Gönczy, 2008; Knoblich, 2008).

How does GPB-1 depart from the cell membrane? Our findings suggest that GPB-1 is not endocytosed but instead translocates to the cytoplasm before entering the endosomal network. First, our FRAP analysis indicates that GPB-1 is internalized at comparable rates across the cell cycle (Fig. 3D), whereas the rate of endocytosis varies across the cell cycle in the early embryo (Nakayama et al., 2009). Second, we found that levels of GPB-1 at the cell membrane do not increase upon
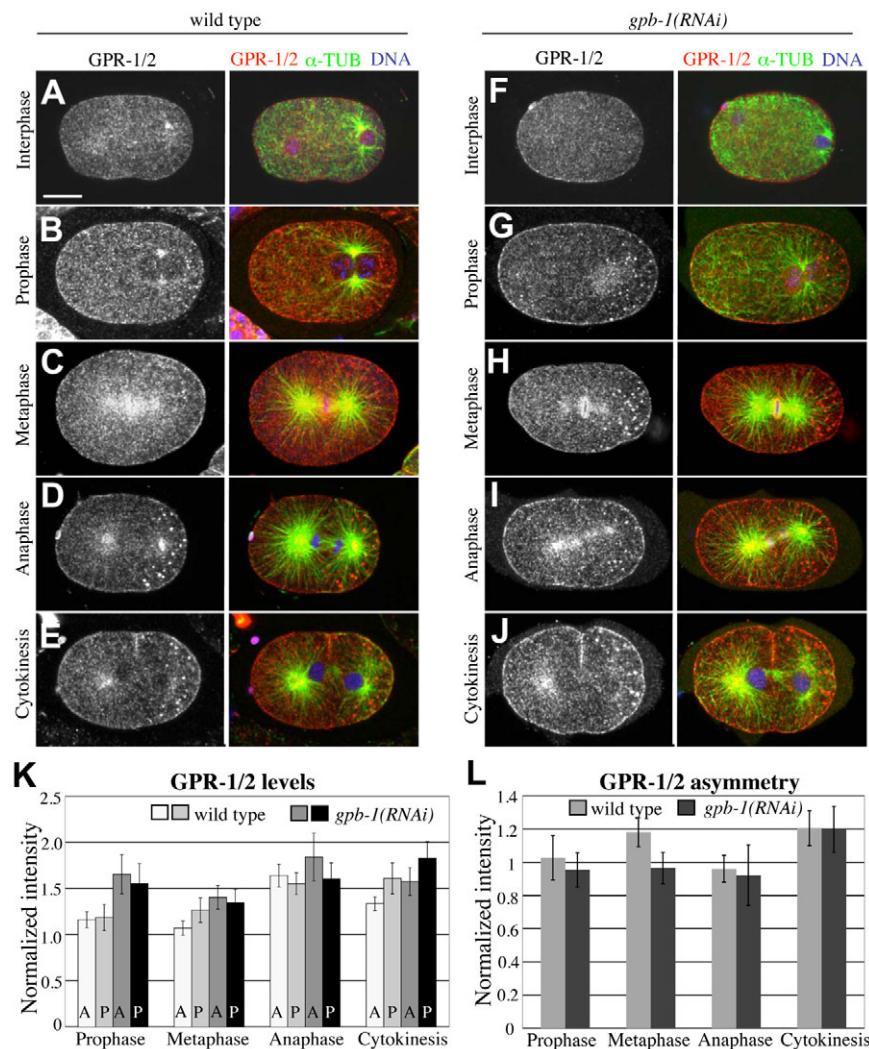

Fig. 6. GPB-1 is important for the temporal and spatial regulation of GPR-1/2. (**A-J**) Wild-type (A-E) and *gpb-1(RNAi)* (F-J) *C. elegans* embryos stained for GPR-1/2 (shown alone in left panels and in red in merges) and α-tubulin (green in merges). Note that the small foci located in the embryo posterior (particularly visible in D,E,H,J) do not appear to correspond to GPR-1/2 as they are still present in *gpr-1/2(RNAi)* embryos (data not shown). Scale bar: 10 μm. (**K**) Normalized GPR-1/2 fluorescence intensity at the anterior (A) and posterior (P) cell membrane in wild-type and *gpb-1(RNAi)* embryos. Error bars represent s.e.m. For wild-type prophase *n*=7, metaphase *n*=10, anaphase *n*=16, cytokinesis *n*=25; for *gpb-1(RNAi)* prophase *n*=12, metaphase *n*=12, anaphase *n*=11, cytokinesis *n*=20. See Table S2 in the supplementary material for actual values and statistical analysis. A value of 1 on the *y*-axis corresponds to an equal intensity of cortical and cytoplasmic GPR-1/2. Note that the difference between the levels of GPR-1/2 on the posterior and on the anterior cell membrane is less pronounced with the antibody utilized here than that employed in a previous study (Colombo et al., 2003). (**L**) Ratio of posterior to anterior normalized GPR-1/2 fluorescence intensity in wild-type and *gpb-1(RNAi)* embryos. Number of embryos analyzed as in K. Error bars represent s.e.m. A value of 1 on the *y*-axis denotes equal cortical GPR-1/2 levels at the anterior and posterior cortex. See Table S2 in the supplementary material for actual values and statistical analysis.

disruption of the endocytic factors dynamin and RAB-5. These findings indicate that GPB-1 enters the endosomal pathway after internalization has occurred, en route to the recycling endosome. Interestingly, recycling is curtailed during mitosis in mammalian cells (Boucrot and Kirchhausen, 2007), raising the possibility that an analogous phenomenon is at play in *C. elegans* embryos. This could provide an explanation for the accumulation of GPB-1 punctae during mitosis, reflecting the transient trapping of GPB-1 in the recycling compartment and resulting in the concomitant diminution of the cell membrane pool.

Gβ contributes to the temporal regulation of force generators

Depletion of the Gβγ subunits GPB-1 or GPC-2 results in a loss of the temporal regulation of force generators, as exaggerated forces are apparent starting in prophase in such embryos (Afshar et al., 2004; Tsou et al., 2003). How might GPB-1 regulate the timing of force generation? Careful examination of wild-type embryos revealed that GPB-1 levels at the cell membrane are high initially, including in prophase (Fig. 7A). Thereafter, cell membrane GPB-1 levels are lower during mitosis (Fig. 7B). In accordance with the cell membrane levels of GPB-1 being important for setting those of GPR-1/2, the distribution of cell membrane GPR-1/2 is roughly reciprocal to that of GPB-1 across the cell cycle, being lower during prophase than during mitosis. This reciprocal relationship is not absolute, however. Thus, whereas GPB-1 is similarly low during metaphase and anaphase (see Fig. 1F), overall GPR-1/2 levels are higher during anaphase (see Fig. 6K). This is in line with the fact that components other than GPB-1, such as PPH-6, CSNK-1, LET-99 and perhaps others, also contribute to regulating GPR-1/2 distribution at the cell membrane.

Polarity, asymmetric trafficking and Gβγ regulation

One of the key open questions in the study of asymmetric spindle positioning concerns the mechanisms by which polarity cues ensure the asymmetric localization of cortical force generators. Previous work showed that GPB-1 does not alter the asymmetry of GPR-1/2 in late anaphase and telophase (Afshar et al., 2004; Tsou et al., 2003). Here, we performed detailed quantification of GPR-1/2 levels at the anterior and posterior cortex across the cell cycle and found that GPB-1 plays an important role in mediating GPR-1/2 asymmetry during metaphase. The symmetric GPR-1/2 distribution in *gpb-1(RNAi)* embryos is compatible with the observation that upon GPB-1 depletion, the net pulling forces that act on the two spindle poles are equal during the anaphase that follows (Afshar et al., 2004). Nevertheless, the first division of *gpb-1(RNAi)* embryos is unequal, presumably because the spindle assembles at the posterior owing to prior aberrant centration/rotation (Afshar et al., 2004; Tsou et al., 2003).

What is the link between polarity cues and GPB-1? The anterior PAR polarity components PAR-6/PKC-3 and CDC-42 regulate intracellular trafficking, including recycling of clathrin-independent cargo (Balklava et al., 2007). In fact, the asymmetric distribution of dynamin, early endosomes and recycling endosomes is under the control of anterior PAR proteins (Andrews and Ahringer, 2007; Balklava et al., 2007; Nakayama et al., 2009), and overall intracellular trafficking is enriched on the anterior side (Nakayama et al., 2009). However, whether such an asymmetry holds true for specific effector cargoes implicated in asymmetric spindle positioning was not known prior to our work.

Our studies reveal that GPB-1 trafficking occurs in an asymmetric manner during mitosis, being more pronounced on the anterior side. First, we found that intracellular vesicles containing GPB-1 have a propensity to accumulate on the posterior side in wild-type embryos during mitosis, which is indicative of less pronounced trafficking on that side. Second, the asymmetry in GPB-1 trafficking is revealed in a most dramatic manner when trafficking is impaired following dynamin or RAB-5 disruption, which results in the accumulation of intracellular punctae primarily on the anterior side. Importantly, we found that the asymmetry in GPB-1 trafficking is lost upon inactivation of A-P polarity cues. Interestingly, however, this asymmetry is maintained in *dyn-1(RNAi)* embryos, in which the maintenance but not the establishment phase of A-P polarity is affected (Nakayama et al., 2009). This suggests that the asymmetry of GPB-1 trafficking is under the control of A-P polarity specifically during the establishment phase. Collectively, these findings indicate that polarity cues regulate GPB-1 trafficking through the endosomal network. Whereas a general impairment in recycling during mitosis may contribute to the overall endosomal accumulation of GPB-1, this might be counteracted on the anterior side specifically by the recycling-promoting PAR complex proteins PAR-6/PKC-3 and CDC-42.

Asymmetric intracellular trafficking is also important during the asymmetric division of *Drosophila* sensory organ precursors, in this case for fate specification (Coumailleau et al., 2009; Emery et al., 2005; Hutterer and Knoblich, 2005). Our work demonstrates that asymmetric trafficking can also be coupled to spindle positioning, thus enabling the system to rapidly alter the localization of force generators and link cell cycle progression with asymmetric cell division.
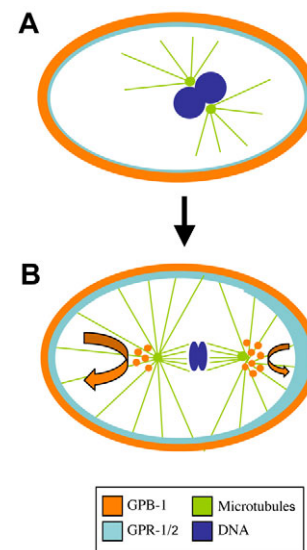

Fig. 7. Model of temporal and spatial distribution of GPB-1 and GPR-1/2. (**A**) During prophase in the one-cell stage *C. elegans* embryo, GPB-1 cell membrane levels are relatively high overall. GPR-1/2 distribution on the cell membrane is reciprocal to that of GPB-1, being relatively low overall. (**B**) During metaphase/anaphase, GPB-1 levels on the cell membrane are lower overall, presumably as a result of the increased accumulation of GPB-1 in early and recycling endosomes. Moreover, trafficking is more pronounced on the anterior side (left), such that GPB-1 tends to accumulate in endosomal vesicles more on the posterior side (right). Less pronounced trafficking on the posterior side might lead to the accumulation of more GPR-1/2 on the cell membrane on that side.

Gβγ trafficking may modulate the availability of Gα subunits for force generation

Heterotrimeric G protein subunits control asymmetric cell division in other systems, including *Drosophila* neuroblasts and mammalian neural progenitors (reviewed by Gönczy, 2008; Knoblich, 2008). In *Drosophila* neuroblasts, the Gα proteins themselves are asymmetrically localized, whereas in mammalian neural progenitor cells Gβ is asymmetrically localized. In the one-cell stage *C. elegans* embryo, by contrast, no asymmetry has been reported for either Gα subunits or Gβ during mitosis (Afshar et al., 2004; Afshar et al., 2005). How could such seemingly symmetric distributions lead to an asymmetry of GPR-1/2 at the cell membrane? Although we cannot exclude the possibility that A-P polarity cues regulate GPR-1/2 asymmetry independently of the asymmetry in GPB-1 trafficking, our correlative data lead us to propose the following working model (Fig. 7). We speculate that differential trafficking of Gβγ proteins on the anterior and posterior sides modulates the availability of free Gα subunits to bind GPR-1/2. Our observation that GPB-1 accumulates more around the posterior aster during mitosis suggests that, transiently, less GPB-1 is available at the posterior, potentially allowing more Gα subunits to bind GPR-1/2 on that side. In summary, the asymmetry in GPR-1/2 distribution at the cell membrane during mitosis could arise from an asymmetry in GPB-1 association with Gα subunits under the control of PAR-dependent asymmetric trafficking. Perhaps such an asymmetry in GPB-1 trafficking serves a similar function as the asymmetric distribution of Gα or Gβγ proteins in other instances of asymmetric cell division: that of achieving an asymmetry in the distribution of force generators located at the cell membrane.

Competing interests statement
The authors declare no competing financial interests.

Supplementary material
Supplementary material for this article is available at
http://dev.biologists.org/lookup/suppl/doi:10.1242/dev.063354/-/DC1

References
Afshar, K., Willard, F. S., Colombo, K., Johnston, C. A., McCudden, C. R., Siderovski, D. P. and Gönczy, P. (2004). RIC-8 is required for GPR-1/2-dependent Galpha function during asymmetric division of *C. elegans* embryos. *Cell* **119**, 219-230.

Afshar, K., Willard, F. S., Colombo, K., Siderovski, D. P. and Gönczy, P. (2005). Cortical localization of the Galpha protein GPA-16 requires RIC-8 function during *C. elegans* asymmetric cell division. *Development* **132**, 4449-4459.

Afshar, K., Werner, M. E., Tse, Y. C., Glotzer, M. and Gönczy, P. (2010). Regulation of cortical contractility and spindle positioning by the protein phosphatase 6 PPH-6 in one-cell stage *C. elegans* embryos. *Development* **137**, 237-247.

Allen, J. A., Yu, J. Z., Donati, R. J. and Rasenick, M. M. (2005). Beta-adrenergic receptor stimulation promotes G alpha s internalization through lipid rafts: a study in living cells. *Mol. Pharmacol.* **67**, 1493-1504.

Andrews, R. and Ahringer, J. (2007). Asymmetry of early endosome distribution in C. elegans embryos. *PLoS ONE* **2**, e493.

Audhya, A., Desai, A. and Oegema, K. (2007). A role for Rab5 in structuring the endoplasmic reticulum. *J. Cell Biol.* **178**, 43-56.

Balklava, Z., Pant, S., Fares, H. and Grant, B. D. (2007). Genome-wide analysis identifies a general requirement for polarity proteins in endocytic traffic. *Nat. Cell Biol.* **9**, 1066-1073.

Bellanger, J. M. and Gönczy, P. (2003). TAC-1 and ZYG-9 form a complex that promotes microtubule assembly in C. elegans embryos. *Curr. Biol.* **13**, 1488-1498.

Boucrot, E. and Kirchhausen, T. (2007). Endosomal recycling controls plasma membrane area during mitosis. *Proc. Natl. Acad. Sci. USA* **104**, 7939-7944.

Cheng, N. N., Kirby, C. M. and Kemphues, K. J. (1995). Control of cleavage spindle orientation in Caenorhabditis elegans: the role of the genes par-2 and par-3. *Genetics* **139**, 549-559.

Chisari, M., Saini, D. K., Kalyanaraman, V. and Gautam, N. (2007). Shuttling of G protein subunits between the plasma membrane and intracellular membranes. *J. Biol. Chem.* **282**, 24092-24098.

Clark, S. G., Shurland, D. L., Meyerowitz, E. M., Bargmann, C. I. and van der Bliek, A. M. (1997). A dynamin GTPase mutation causes a rapid and reversible temperature-inducible locomotion defect in C. elegans. *Proc. Natl. Acad. Sci. USA* **94**, 10438-10443.

Colombo, K., Grill, S. W., Kimple, R. J., Willard, F. S., Siderovski, D. P. and Gönczy, P. (2003). Translation of polarity cues into asymmetric spindle positioning in Caenorhabditis elegans embryos. *Science* **300**, 1957-1961.

Coumailleau, F., Furthauer, M., Knoblich, J. A. and Gonzalez-Gaitan, M. (2009). Directional Delta and Notch trafficking in Sara endosomes during asymmetric cell division. *Nature* **458**, 1051-1055.

Couwenbergs, C., Labbe, J. C., Goulding, M., Marty, T., Bowerman, B. and Gotta, M. (2007). Heterotrimeric G protein signaling functions with dynein to promote spindle positioning in C. elegans. *J. Cell Biol.* **179**, 15-22.

Damke, H., Baba, T., van der Bliek, A. M. and Schmid, S. L. (1995). Clathrin-independent pinocytosis is induced in cells overexpressing a temperature-sensitive mutant of dynamin. *J. Cell Biol.* **131**, 69-80.

Emery, G., Hutterer, A., Berdnik, D., Mayer, B., Wirtz-Peitz, F., Gaitan, M. G. and Knoblich, J. A. (2005). Asymmetric Rab 11 endosomes regulate delta recycling and specify cell fate in the Drosophila nervous system. *Cell* **122**, 763-773.

Garcia-Regalado, A., Guzman-Hernandez, M. L., Ramirez-Rangel, I., Robles-Molina, E., Balla, T., Vazquez-Prado, J. and Reyes-Cruz, G. (2008). G protein-coupled receptor-promoted trafficking of Gbeta1gamma2 leads to AKT activation at endosomes via a mechanism mediated by Gbeta1gamma2-Rab11a interaction. *Mol. Biol. Cell* **19**, 4188-4200.

Gönczy, P. (2008). Mechanisms of asymmetric cell division: flies and worms pave the way. *Nat. Rev. Mol. Cell Biol.* **9**, 355-366.

Gönczy, P., Echeverri, C., Oegema, K., Coulson, A., Jones, S. J., Copley, R. R., Duperon, J., Oegema, J., Brehm, M., Cassin, E. et al. (2000). Functional genomic analysis of cell division in C. elegans using RNAi of genes on chromosome III. *Nature* **408**, 331-336.

Gotta, M. and Ahringer, J. (2001). Distinct roles for Galpha and Gbetagamma in regulating spindle position and orientation in Caenorhabditis elegans embryos. *Nat. Cell Biol.* **3**, 297-300.

Gotta, M., Dong, Y., Peterson, Y. K., Lanier, S. M. and Ahringer, J. (2003). Asymmetrically distributed C. elegans homologs of AGS3/PINS control spindle position in the early embryo. *Curr. Biol.* **13**, 1029-1037.

Grill, S. W., Gönczy, P., Stelzer, E. H. and Hyman, A. A. (2001). Polarity controls forces governing asymmetric spindle positioning in the Caenorhabditis elegans embryo. *Nature* **409**, 630-633.

Grill, S. W., Howard, J., Schaffer, E., Stelzer, E. H. and Hyman, A. A. (2003). The distribution of active force generators controls mitotic spindle position. *Science* **301**, 518-521.

Hutterer, A. and Knoblich, J. A. (2005). Numb and alpha-Adaptin regulate Sanpodo endocytosis to specify cell fate in Drosophila external sensory organs. *EMBO Rep.* **6**, 836-842.

Hynes, T. R., Mervine, S. M., Yost, E. A., Sabo, J. L. and Berlot, C. H. (2004). Live cell imaging of Gs and the beta2-adrenergic receptor demonstrates that both alphas and beta1gamma7 internalize upon stimulation and exhibit similar trafficking patterns that differ from that of the beta2-adrenergic receptor. *J. Biol. Chem.* **279**, 44101-44112.

Knoblich, J. A. (2008). Mechanisms of asymmetric stem cell division. *Cell* **132**, 583-597.

Marrari, Y., Crouthamel, M., Irannejad, R. and Wedegaertner, P. B. (2007). Assembly and trafficking of heterotrimeric G proteins. *Biochemistry* **46**, 7665-7677.

Nakayama, Y., Shivas, J. M., Poole, D. S., Squirrell, J. M., Kulkoski, J. M., Schleede, J. B. and Skop, A. R. (2009). Dynamin participates in the maintenance of anterior polarity in the Caenorhabditis elegans embryo. *Dev. Cell* **16**, 889-900.

Nguyen-Ngoc, T., Afshar, K. and Gönczy, P. (2007). Coupling of cortical dynein and G alpha proteins mediates spindle positioning in Caenorhabditis elegans. *Nat. Cell Biol.* **9**, 1294-1302.

Panbianco, C., Weinkove, D., Zanin, E., Jones, D., Divecha, N., Gotta, M. and Ahringer, J. (2008). A casein kinase 1 and PAR proteins regulate

asymmetry of a PIP(2) synthesis enzyme for asymmetric spindle positioning. *Dev. Cell* **15**, 198-208.

Park, D. H. and Rose, L. S. (2008). Dynamic localization of LIN-5 and GPR-1/2 to cortical force generation domains during spindle positioning. *Dev. Biol.* **315**, 42-54.

Praefcke, G. J. and McMahon, H. T. (2004). The dynamin superfamily: universal membrane tubulation and fission molecules? *Nat. Rev. Mol. Cell Biol.* **5**, 133-147.

Praitis, V., Casey, E., Collar, D. and Austin, J. (2001). Creation of low-copy integrated transgenic lines in Caenorhabditis elegans. *Genetics* **157**, 1217-1226.

Saini, D. K., Kalyanaraman, V., Chisari, M. and Gautam, N. (2007). A family of G protein betagamma subunits translocate reversibly from the plasma membrane to endomembranes on receptor activation. *J. Biol. Chem.* **282**, 24099-24108.

Sato, M., Sato, K., Liou, W., Pant, S., Harada, A. and Grant, B. D. (2008). Regulation of endocytic recycling by C. elegans Rab35 and its regulator RME-4, a coated-pit protein. *EMBO J.* **27**, 1183-1196.

Srinivasan, D. G., Fisk, R. M., Xu, H. and van den Heuvel, S. (2003). A complex of LIN-5 and GPR proteins regulates G protein signaling and spindle function in C elegans. *Genes Dev.* **17**, 1225-1239.

Thompson, H. M., Skop, A. R., Euteneuer, U., Meyer, B. J. and McNiven, M. A. (2002). The large GTPase dynamin associates with the spindle midzone and is required for cytokinesis. *Curr. Biol.* **12**, 2111-2117.

Timmons, L. and Fire, A. (1998). Specific interference by ingested dsRNA. *Nature* **395**, 854.

Tsou, M. F., Hayashi, A. and Rose, L. S. (2003). LET-99 opposes Galpha/GPR signaling to generate asymmetry for spindle positioning in response to PAR and MES-1/SRC-1 signaling. *Development* **130**, 5717-5730.

Vida, T. A. and Emr, S. D. (1995). A new vital stain for visualizing vacuolar membrane dynamics and endocytosis in yeast. *J. Cell Biol.* **128**, 779-792.

Zwaal, R. R., Ahringer, J., van Luenen, H. G., Rushforth, A., Anderson, P. and Plasterk, R. H. (1996). G proteins are required for spatial orientation of early cell cleavages in C. elegans embryos. *Cell* **86**, 619-629.